

Original article

# Comparing the Dosimetric Properties of 6 MeV to 9 MeV electron beam of Varian Clinac 2100C/D Linear Accelerator Using OMEGA-BEAMnrc Monte Carlo Code System

Ibrahim Othman\*<sup>ID</sup>, Ibrahim Salim

Department of Radiation Technology, Faculty of Medical Technology, Aljufra University, Houn, Libya

## ARTICLE INFO

Corresponding Email. [o.attia@zu.edu.ly](mailto:o.attia@zu.edu.ly)

Received: 30-04-2023

Accepted: 21-10-2023

Published: 29-12-2023

**Keywords.** Radiation Dosimetry, Monte Carlo OMEGA BEAMnrc, Phase Space File, Dose Profiles, Isodose Curves.

This work is licensed under the Creative Commons Attribution International License (CC BY 4.0).

<http://creativecommons.org/licenses/by/4.0/>

## ABSTRACT

**Aims.** This work shows the differences of 6MeV and 9MeV electron beam modes of Varian Clinac 2100CD Linear accelerator (Linac) by investigating their dosimetric data. **Methods.** The treatment planning used here is the Monte Carlo (MC) OMEGA-BEAMnrc code system, widely used to improve different equipment's used in radiation therapy. In the present work, the above mentioned Linac was simulated using BEAMnrc MC code system to produce 10x10cm phase space file of 6MeV electron beam. The produced spectra of the beam phase-space and that provided by the International Atomic Energy Agency (IAEA) for the electron beam of 10cmx10cm field of view were modeled, simulated and finally analyzed using BEAMdp. The beam properties studied here are, the fluence, energy fluences, mean energy and angular and spectral distribution of beam components, photons, electrons, positrons and total sum (all components). The produced electron beams were transported in water phantom using DOSXYZnrc code and the central-axis absorbed dose, the beam profiles, and the isodose curves were calculated. The central axis depth-dose curves, dose profiles and isodose curves of the electron beams in water phantom were analyzed using DOSXYZnrc, STATDOSE and DOSXYZ\_SHOW code. **Results.** The results of this study for 6 MeV beam were compared with that previously published for 9 MeV beam. This study showed that the depth at maximum dose  $d_{max}$  for 9MeV beam is higher than that for 6MeV while both profiles have the same trend. The OMEGA-BEAMnrc code system can create the phase space data files accurately and are similar to those provided by IAEA data. **Conclusion.** Omega Beam Code system can simulate the clinical linear accelerator to produce electron beam which can be used to generate accurate MC dose distributions in water phantom or in patients for the sake of equipment improvements in radiation therapy and for radiation dosimetry purposes.

**Cite this article.** Othman I, Salim I. Comparing the Dosimetric Properties of 6 MeV to 9 MeV electron beam of Varian Clinac 2100C/D Linear Accelerator Using OMEGA-BEAMnrc Monte Carlo Code System. *Alq J Med App Sci.* 2023;6(2):890-902. <https://doi.org/10.5281/zenodo.10827506>

## INTRODUCTION

In External Radiation Therapy (ERT), precise dose has to be delivered to the patient's tumor accurately [1-5]. Prior to treatment radiation exposure, a computerized treatment plan is achieved to ensure accurate dose delivery to the desired

target [6-9]. The beam is arranged so that the dose to the target tumor is maximized while it must be minimized to the surroundings. Varian linear accelerators (Palo Alto, CA) are often accompanied by the Varian Eclipse™ treatment planning system, which uses the AAA convolution-superposition algorithm [10]. The OMEGA-BEAMnrc and the DOSXYZnrc along with other code system utilities, sponsored by the National Research Council Canada (NRCC) are widely used Monte Carlo package for simulating, in much more details, radiotherapy beams and calculating dose distributions in phantoms or in patients [11-13]. The BEAMnrc code system was designed to simulate radiation beams from a medical linear accelerator, including Co-60 and low energy x-rays machine. The model of treatment head was built in the BEAMnrc from the so-called Component Modules (CM) which accurately simulates various parts of the treatment head. The result of BEAMnrc head simulation is the production of beam phase space file. The phase space file is a collection of representative pseudo-particles emerging from a radiation therapy treatment source along with their properties that include particle type, energy, position, direction, progeny and statistical weight. The DOSXYZnrc code use the BEAMnrc output phase-space file to calculate dose distributions in a phantom to give three-dimensional 3D dose distributions in a defined volume when irradiated. It can use an inhomogeneous phantom by defining the properties of each individual volume element. Both codes are based on the well-known Electron-Gamma-Shower (EGSnrc) code system, running on Linux/Unix operating system. Provided, FORTRAN and C++ suite of compilers along with other utilities have to exist in order to achieve the simulation. Tumors can be treated with a one or two field, the so-called conventional radiotherapy. In the 3D Conformal Radiation Therapy, enhanced imaging technology of the body allows for programming of treatment beams. This is done by treating with large numbers of beams. Each is shaped with a Multi Leaf Collimator (MLC). In recent years, the Intensity Modulated Radiation Therapy (IMRT) is considered as one of the latest advancements in radiation therapy. This new approach allows for dose sculpting and even distribution of delivery for precise uniform treatment. In this technique, the MLC moves and modulates the radiation as the Linac treats the patient [14-18].

Objectives: In previous studies, we presented that, for ERT and Brachytherapy, EGSnrc system along with its different tools has showed its advancements in dose calculations in general and radiotherapy planning in particular [19-23]. In the present work, we extended the simulation using BEAMnrc code to include the 6 MeV electron beam of Varian Clinac 2100C/D Linac to produce the phase space file at a Source to Surface Distance SSD=100 cm. This position is just above either the patient or the phantom surface. The resulted phase space beam was compared with that of IAEA data for further investigations of the dosimetric properties.

## METHODS

### *Radiotherapy Treatment Planning*

The OMEGA-BEAM code system used in this study was the latest (Version 2023) release. The standard system was installed on Intel(R) Core(TM) i7-4770 8-CPU @ 3.40GHz 8-Threads processor running Debian GNU Linux workstation along with the GNU suite of compilers. The geometry models were based on electron beam from Varian Clinac 2100C/D medical linear accelerator. Common components in the geometry model for the beams are: primary collimator, vacuum exit window, dual ionization chamber, lead shielding plate, field mirror with its frame, jaws, fully retracted multileaf collimator and light field reticle. Above primary collimator there is a two-layer x-ray target in photon beam and vacuum in electron beam. Between vacuum exit window and dual ionization chamber there is a flattening filter in photon beam and dual scattering foils in electron beam. Below light field reticle there is air to the level of phantom surface, but in electron beam there is an electron applicator with square Cerrobend™ cutout. In electron beam model, in this work, the nominal energy is 6 MeV. The particle data is gathered to phase space files at SSD=100 cm for beam model of electron applicator size 10x10 cm<sup>2</sup>. The EGSnrc parameters are: E<sub>CUT</sub>=A<sub>E</sub>=0.521 MeV, P<sub>CUT</sub>=A<sub>P</sub>=0.01 MeV; Electron-step algorithm=PRESTA-II; Spin effects=On, Brems angular sampling=KM; Brems cross sections=NIST; Bound Compton scattering=On; Pair angular sampling=KM; Photoelectron angular sampling=KM; Rayleigh scattering=On, Atomic relaxations=On; Electron impact ionization = On; Photon cross sections=xcom

The Monte Carlo code system BEAMnrc was used to model the high energy electron Linac head and consequently the full beam phase space file was produced. Phase space file that resulted from the present simulation and that provided by IAEA are investigated for accuracy checkup. Analysis of the phase space were done using BEAMDP code. The full beam phase space file was transported in water phantom using DOSXYZnrc to produce the 3D dose distributions required for dose profile representation. Calculations of the transmitted dose in the water phantom were investigated. Analysis of the data and isodose curves were done and represented using, STATDOSE and DOSXYZ\_SHOW codes.

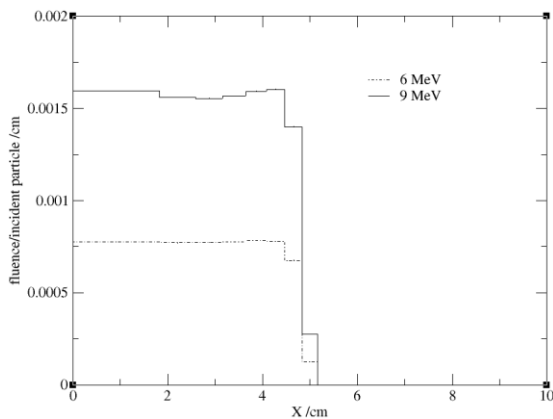
For electron beam, the number of histories was  $5 \times 10^8$ . The sizes of calculation voxels were adapted to be small in regions of high dose gradients and vice versa. In horizontal plane (X- axis) sizes varied between 0.2 to 1 cm in electron beam model, being the smallest near “profile shoulder” and penumbral region. The horizontal voxels around beam central axis were combined to larger voxels to produce statistically more reliable calculation results. In vertical direction (Z-axis) sizes varied between 0.1 to 1.0 cm, being the smallest near the surface, in dose build-up region, around the depth of dose maximum (dmax) and in the end of linear dose build-down region. Statistical uncertainties for the calculated dose values for each voxel were below 0.002 %, being slightly higher near the surface in Z axis and in the ends of profiles. The EGSnrc parameters are the same as in first phase simulations. Calculated vertical dose distributions were normalized to percentage depth dose (PDD) curves and also to unity. In Monte Carlo simulation of high energy medical linear accelerators (Linacs), important components are to be controlled in details in order to shape the output beam [24-27].

## RESULTS AND DISCUSSIONS

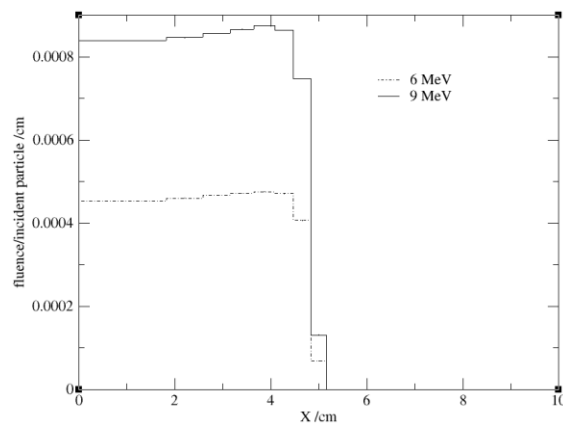
Both BEAMnrc and IAEA phase space file at 100 cm SSD and 10x10cm field of view for Varian Clinac 2100C Linac were examined and investigated using BEAMdb code. 6MeV electron beam characteristics including both particle and energy fluences, spectral and angular distributions, and mean energy data of electrons, positrons, photons and total particles were extracted. The examined data were analyzed and represented using the linear and non-linear regression analysis software GRACE package. It performs both linear and nonlinear least-squares fitting to arbitrarily complex user-defined functions, with or without constraints.

### *Particle Fluence Versus Position*

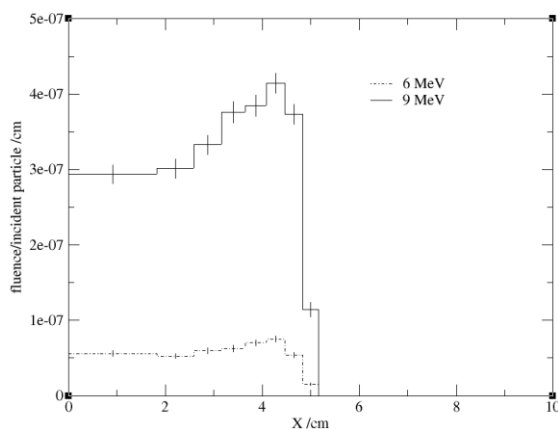
A radiation field at any point P can be quantified by the physical non-stochastic quantity called fluence, which is usually expressed in units of  $m^{-2}$  or  $cm^{-2}$ , and is given by the relation:  $\Phi = dN/da$ . Where, dN is the number of particles (in this work, photons or electrons) striking an infinitesimal sphere with a great circle area, da, surrounding point P. The particles included in  $\Phi$  may have any direction, but correspond to one type of radiation, so that photons and electrons are counted separately. Figure 1 shows the particle fluence versus position x for 6MeV compared with previously published 9MeV electron beam. The data for all particles (a), electrons (b), positrons (c) and photons (d) are represented. In general, the particle fluence of 6 MeV electron beam is less than that of 9 MeV beam. All the graphs show the same trend except that the number of positrons is quite low compared to the number of electrons and photons. This is quite clear from the y-axes scales where the beam is mainly electrons and photons with some positrons scattered from the collimator parts. The high error bar in the positron graph is due to poor count rate.



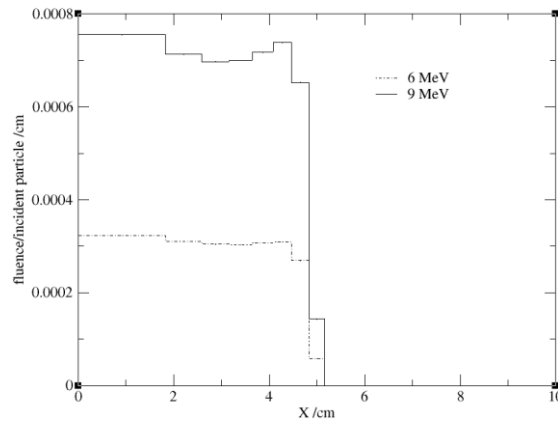
(a) Fluence of all



(b) Fluence of electrons



(c) Fluence of positrons

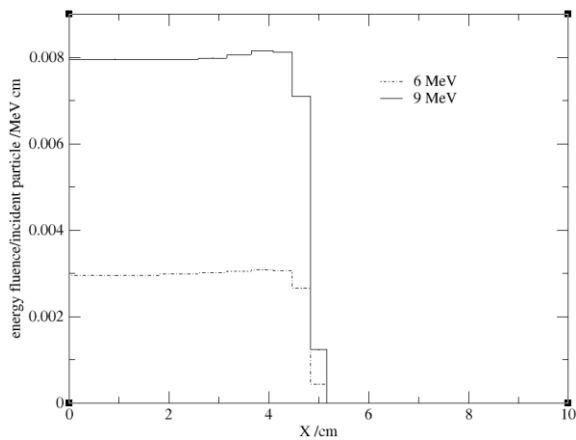


(d) Fluence of photons

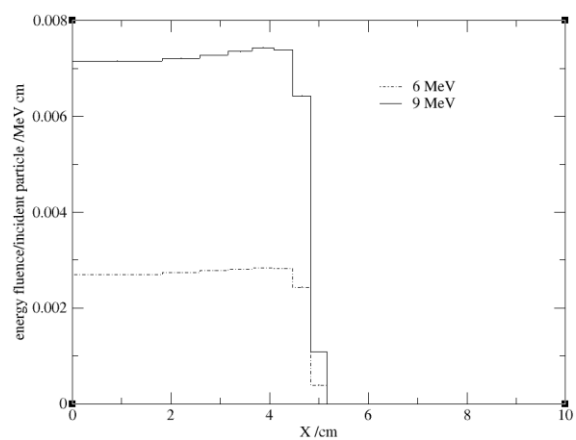
Figure 1. Total (a), electrons (b), positrons (c) and photons (d) fluence are represented as functions of distance  $x$ .

### Energy Fluence Versus Position

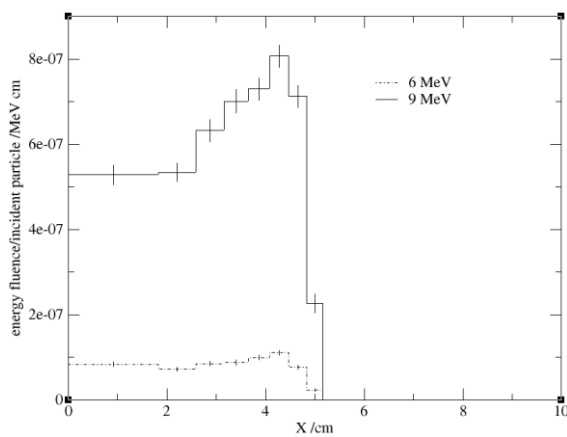
The energy fluence is the sum of radiant energy of each particle that strikes the infinitesimal sphere:  $\Psi = dR/da$ . Where,  $dR$  is the differential of the radiant energy  $R$  (kinetic energy of massive particles and energy of photons) that impinges on the infinitesimal sphere with a great circle area,  $da$ . The SI unit of energy fluence is joules per square metre ( $J/m^2$ ). If the radiation field is composed of particles with the same energy  $E$ , the energy fluence is related to the particle fluence by:  $\Psi = E \Phi$ . Figure 2 shows the particle energy fluence versus position  $x$  for 6MeV compared with previously published 9MeV electron beam. The data for all particles (a), electrons (b), positrons (c) and photons (d) are presented. Energy fluence for 9MeV beam is higher than that for 6MeV one. All the graphs show again the same trend except that the number of positrons is quite low compared to the number of electrons and photons. This is quite clear from the y-axes scales where the beam is mainly electrons and photons with some positrons scattered from the collimator parts. Notice the high standard deviation in the positron graph due to its poor count rate statistics.



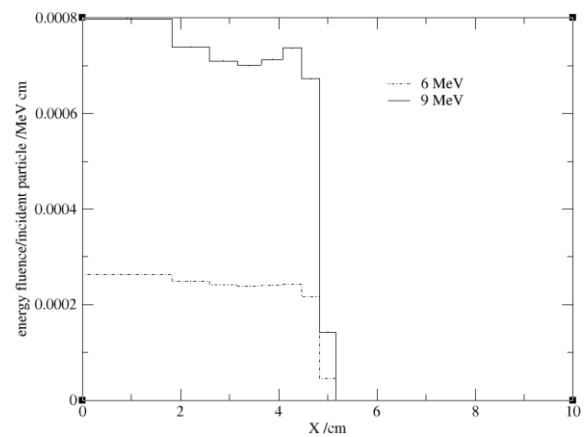
(a) Energy fluence of all



(b) Energy fluence of electrons



(c) Energy fluence of positrons

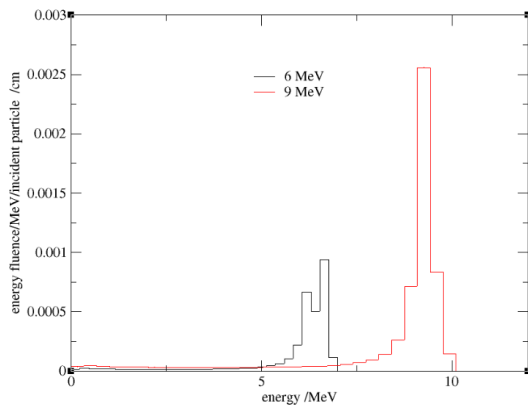


(d) Energy fluence of photons

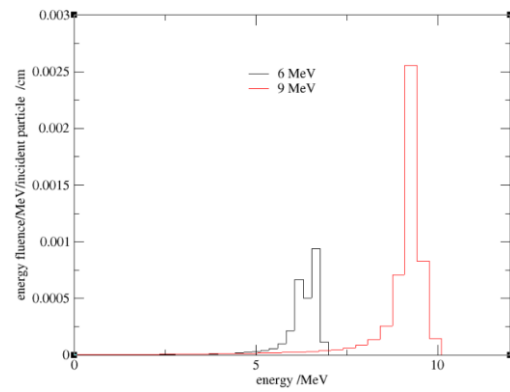
**Figure 2.** Total (a), electrons (b), positrons (c) and photons (d) energy fluence are represented as functions of distance  $x$ .

### Energy Fluence Distribution

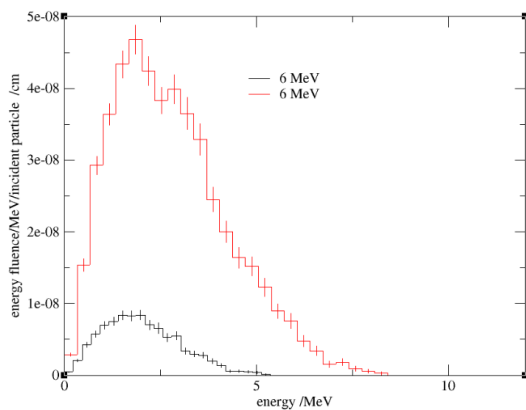
Figure 3 shows the particle energy fluence distribution for; all particles (a), electrons (b), positrons (c) and photons (d). For 6 and 9 MeV beams respectively, the energy fluence distribution of electron gives peak at energy around 6 and 9 MeV while that of both photons and positrons gives peak around 2 MeV. The maximum energy fluence of positrons are quite low compared to the number of electrons and photons. This is quite clear from the y-axes scales where the beam is mainly electrons and photons with some positrons scattered from the collimator parts. Notice the high standard deviation in the positron graph due to its poor count rate statistics.



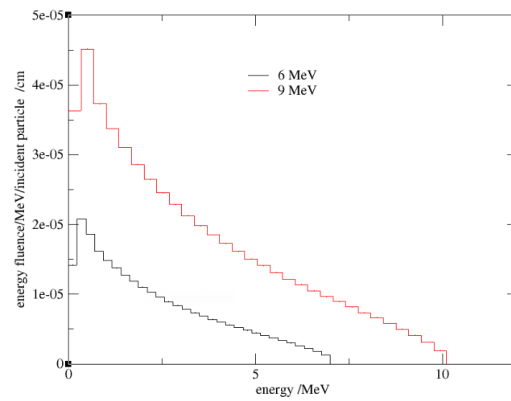
(a) Energy fluence distribution of all



(b) Energy fluence distribution of electrons



(c) Energy fluence distribution of positron

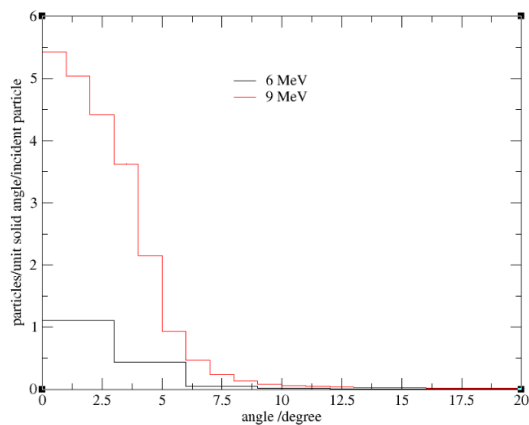


(d) Energy fluence distribution of photons

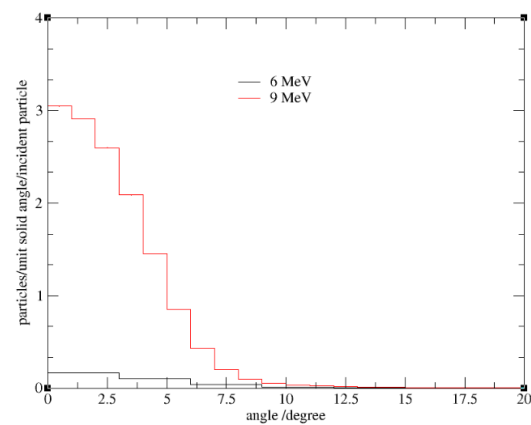
**Figure 3. Total (a), electrons (b), positrons (c) and photons (d) energy fluence distribution are represented as functions of energy bins.**

### Angular Distribution

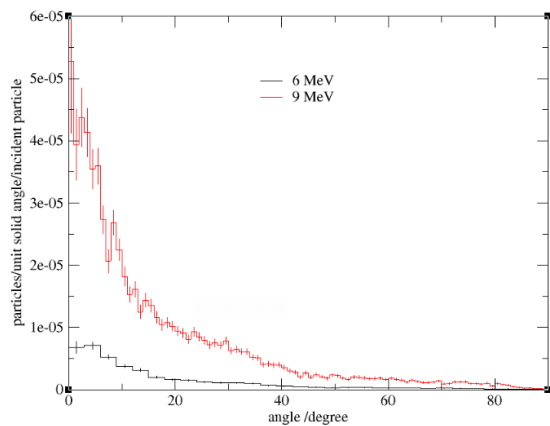
Figure 4 shows the particle angular distribution for; all particles (a), electrons (b), positrons (c) and photons (d). All the particles were scored in solid angular bins and the graphs do not show the same trend where there are a number of positrons scattered by the collimator parts with angles sometimes reach 30o-40o compared to about 4o angles of electrons and photons.



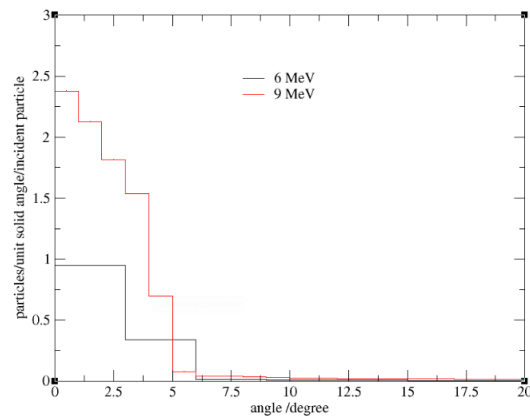
(a) Solid angular distribution of all



(b) Solid angular distribution of electrons



(c) Solid angular distribution of positrons



(d) Solid angular distribution of photons

**Figure 4.** Total (a), electrons (b), positrons (c) and photons (d) angular distribution are represented as functions of solid angle in degrees.

### Mean Energy Distribution

Mean Energy is the ratio of the total particle energy to the total number of particles scored in a spatial bin of equal area. The mean energy in a bin,  $\bar{E}$  is given by:  $\bar{E} = \sum_i (wtE)_i / \sum_i wti$ . where  $(wtE)_i$  is the sum of (particle weight  $w_t$  multiplied by particle energy  $E$  from the  $i$ -th primary history and  $wti$  is the sum of particle weights from the  $i$ -th primary history. When this option is chosen BEAMDP will process the phase-space data and generate a mean energy data file with format suitable for grace plots. The user will be asked to select field types, field dimensions, particle type, graph options, phase-space file etc... to be processed and the data file for outputs. Each data point in the data file represents the mean energy of the particles scored within a given spatial bin for the particle types. Figure 5 shows the particle mean energy versus position  $x$  for 6MeV compared to previously published 9MeV electron beam. The data for all particles (a), electrons (b), positrons (c) and photons (d) are presented. Electron mean energies are about 6 and 8.5 MeV for 6 and 9 MeV beams, respectively. Photon mean energies are about 0.8 and 1.1 MeV for 6 and 9 MeV beams, respectively. Positron mean energies are about 1.5 and 1.75 MeV for 6 and 9 MeV beams, respectively. In general, mean energy is highest at the center of the beam with radius of about 5cm for all particles. Beyond 5 cm radius the mean energy value drops down toward zero value for 9 MeV beam which indicates the boundary of beam fields while the mean energy drops toward

zero value beyond a 6 cm radius. This means that the field size for 6 MeV beam is about 1cm wider than that of 9 MeV beam.

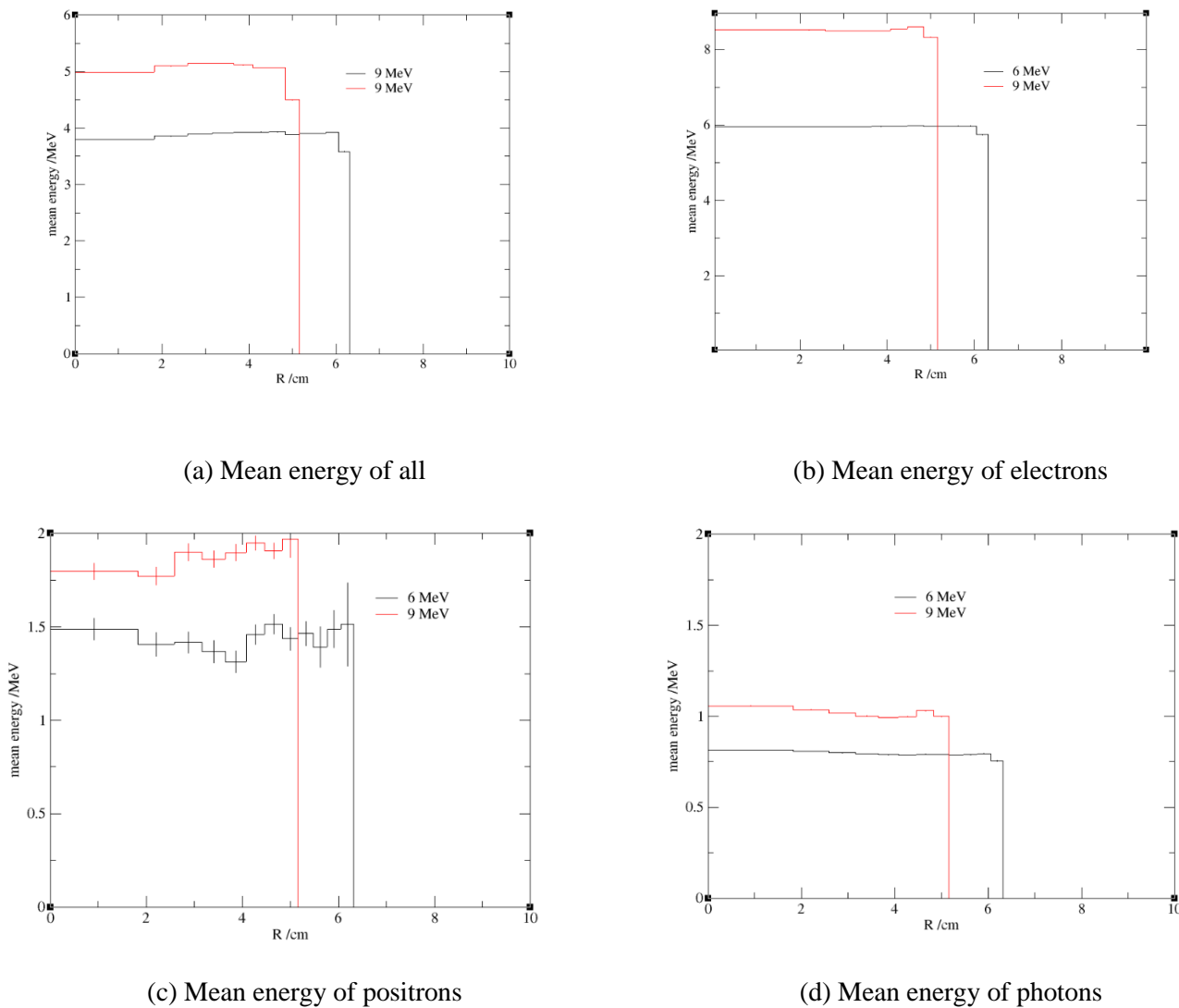
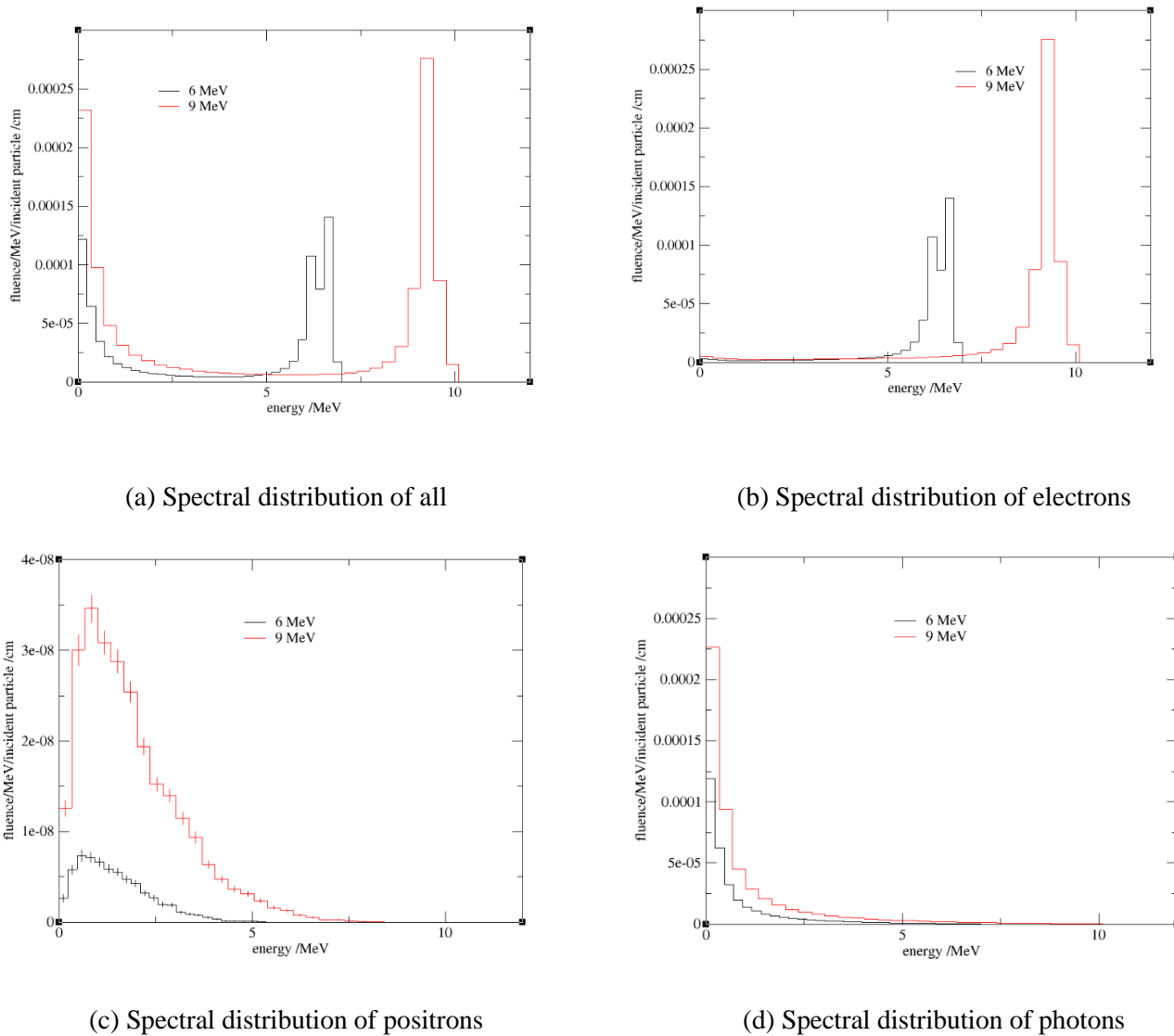


Figure 5. Total (a), electrons (b), positrons (c) and photons (d) mean energy are represented as functions of distance  $x$

### Spectral Distribution

BEAMDP reads the parameters of the phase-space particles and bins particles according to their energy the so-called spectral distribution. Within a bin, particles are grouped according to primary history. Assuming that a phase-space data file contains particles from  $N$  primary histories, the mean of a quantity of interest  $E$  (energy) in a bin, can be calculated as:  $\bar{E} = \sum N E_N / N$ . When this option is chosen, BEAMDP will process the phase-space data and generate a spectral data file with format suitable for grace plots. The user will be asked to select field types and field dimensions, energy range, particle type, the names of the phase-space file etc... to be processed for outputs graph. The phase space file were used to obtain the spectral distribution of 10cmx10cm field of view for both 6 MeV and 9 MeV electron beams as shown in Figure 6. The figure shows that the electrons are the main component of both beams and the least are the positrons. The less is the number of positrons in the produced beam, the higher is the scattering of points of the spectral curve. This is due to the poor statistics of the very small number of positrons within the scored regions. This is expected for a electron beam of any linear accelerator because of the interactions of the emerging x-ray photons with the collimators. For 6

MeV electron beam, the spectral peak maximum is around 6 MeV and around 1-2 MeV for positrons and photons. For 9 MeV electron beam, the spectral peak maximum is around 9 MeV and around 1-2 MeV for positrons and photons.



**Figure 6.** Total (a), photon (b), electron (c) and positron (d) spectral distribution are represented as functions of energy bins.

### Off-Axis Ratios (OAR) and Beam Profiles

Dose distributions along the beam central axis give only part of the information required for an accurate dose description inside the patient. Dose distributions in two (2-D) and three (3-D) dimensions are determined with central axis data in conjunction with off-axis dose profiles. Combining a central axis dose distribution with off-axis data results in a volume dose matrix that provides 2-D and 3-D information on the dose distribution. The off-axis ratio (OAR) is usually defined as the ratio of dose at an off-axis point to the dose on the central beam axis at the same depth in a phantom. The IAEA phase space file of 6MeV Varian 2100C/D Clinac linear accelerator was used to score the depth dose distribution curves in water phantom at 100cm SSD using the DOSXYZnrc code system and compared with that of previously studied 9MeV electron beam [19]. The beam field of view is 10x10cm. The data were analyzed and presented using STATDOSE code with the aid of Grace software. Figure 7(a, b) shows the dose curves at four different xy plane areas [(0,0); (3,3); (4,4) and (5,5)] measured in cm, in the direction off the central axis where the depth is set in the z-direction. The maximum dose Dmax moves toward higher depths as the xy area increases. Figure 7(c, d) shows the dose profile of the beam around the central axis. It shows the dose fall off at 5cm on either side which is the radius of the 10cmx10cm field

of view of the photon beam. Mega-voltage beam profiles consist of three distinct regions: central, penumbra and umbra. The central region represents the central portion of the profile extending from the beam central axis to 5cm in this study as illustrated in figure 7(c, d). In the penumbral region of the dose profile the dose changes rapidly and depends also on the field defining collimators Umbra is the region outside the radiation field, far removed from the field edges which is beyond 5cm in this study.

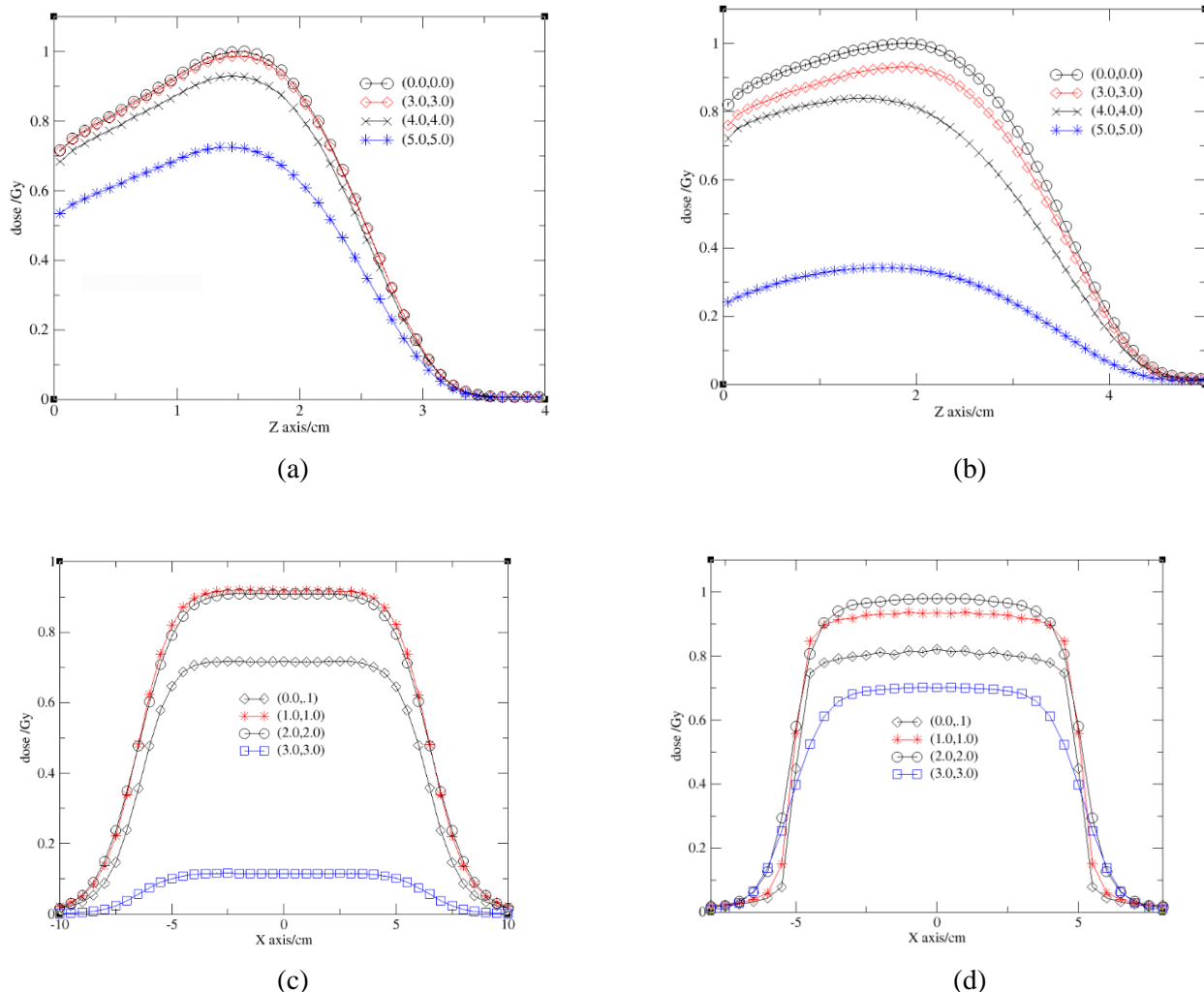
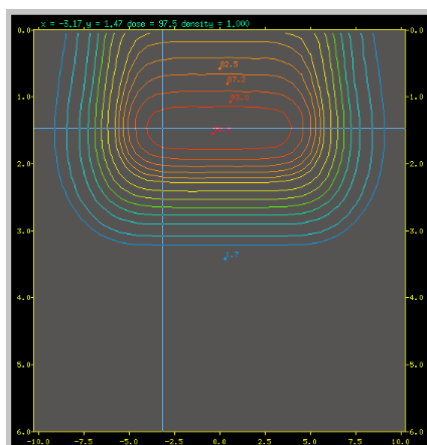


**Figure 7.** Depth and radial dose distribution of 10cmx10cm Varian Clinac 2100CD electron beam in water phantom. Figures (a) and (b) refer to depth doses of 6MeV and 9MeV at some (the legend) x and y values. Figures (c) and (d) refer to radial doses of 6MeV and 9MeV at some (the legend) x and y values.

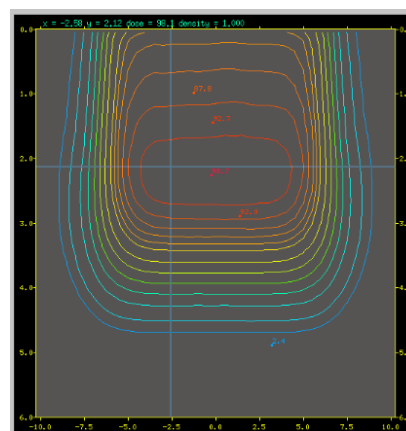
### Isodose Curves

An isodose chart for a given single beam consists of a family of isodose curves usually drawn at regular increments of Percentage Depth Dose (PDD). The dose then could be normalized in either Source to Surface Distance set-up (SSD) or in Source to Axis Distance (SAD) set-up. The isodose curves and surfaces are usually drawn at regular intervals of absorbed dose and are expressed as a percentage of the dose at a specific reference point. In the present work, the DOSXYZ\_SHOW software was used to display the dose data with the created water phantom file during the simulation. Figure 8 shows the isodose charts for Varian 6MeV 2100C/D Clinac linear accelerator electron beam in water phantom compared with that for 9MeV beam [19]. It shows an SSD set-up ( $A = 10 \times 10 \text{ cm}^2$ ; SSD = 100 cm). Figure 8(a,b), on one hand, shows xz planner view for both electron beams where the depth of maximum dose  $d_{max}$  for 9MeV is clearly greater than that of 6MeV beam. On the other hand figure 8(c,d) shows the xy planner view for 6MeV (depth at slice number 16) and 9MeV (depth at slice number 24). The dose profile behavior for both slices are nearly similar. The

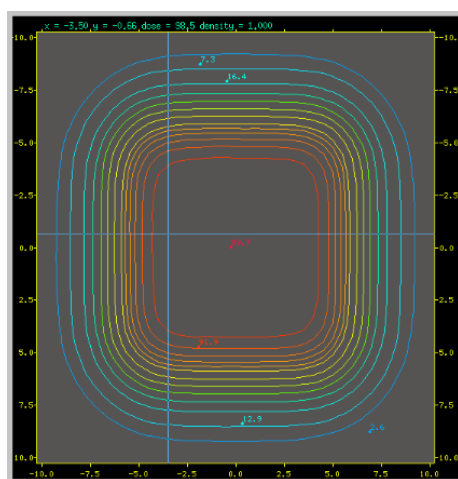
coordinate cross markers in both figures can move everywhere at any position on the image to display the dose information at the top of the images. The isodose curves show that near the beam edges in the penumbra region, the dose decreases rapidly from near 100% to few percent with lateral distance from the beam central axis. This dose fall-off is apparently caused by both the geometric penumbra effect and the reduced side scatter. In umbra region outside the radiation field, far removed from the field edges which is beyond 5cm in this study, the dose is decreased to a minimum of about 1-2%.



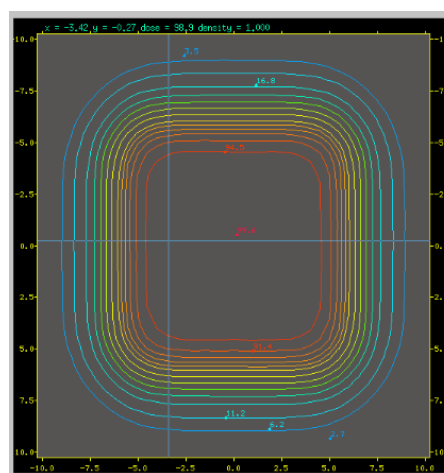
(a)



(b)



(c)



(d)

**Figure 8.** Isodose charts for Varian 9MeV 2100C/D Clinac Linac electron beam in water phantom. It shows an SSD set-up ( $A = 10 \times 10 \text{ cm}^2$ ;  $SSD = 100 \text{ cm}$ ). It shows xz (a, b) and xy (c, d) planner view.

## CONCLUSION

The electron beam of Varian 6MeV 2100C/D Clinac Linac was created using OMEGA BEAM MC code for the sake of comparisons with previously investigated 9MeV electron beam. The accelerator beam spectra at 100cm source to surface distance SSD were produced and analyzed. The depth dose curves and dose profiles for 10cmx10cm beam were scored in water phantom. Planar and volumetric variations in depth doses were displayed by means of isodose curves or isodose surfaces, which connect points of equal dose in a volume of interest to represent the so-called dose contour. This study showed that the depth at maximum dose  $d_{max}$  for 9MeV beam is higher than that for 6MeV one while both profiles

have the same trend. The OMEGA-BEAMMC code system can create the phase space data files accurately which are comparable to those provided by IAEA data. Provided, the produced beam can be used to generate accurate MC dose distributions for electron beams that are produced using clinical high energy Linacs in water phantom or in patients. The dose profiles were represented in a SSD set-up ( $A = 10 \times 10 \text{ cm}^2$ ;  $SSD = 100 \text{ cm}$ ). The isodose curves show that at 5cm near the beam edges in the penumbra region, the dose decreases rapidly from near 100% to about few percent with lateral distance from the beam central axis. This dose fall-off is apparently caused by both the geometric penumbra effect and the reduced side scatter. In umbra region outside the radiation field, far removed from the field edges which is beyond 5cm in this study, the dose is decreased to a minimum of about 1-2 percent.

## REFERENCES

1. Andreo P. Monte Carlo techniques in medical radiation physics. *Phys Med Biol.* 1991 Jul;36(7):861-920.
2. Hartmann Siantar CL, Walling RS, Daly TP, Faddegon B, Albright N, Bergstrom P, Bielajew AF, Chuang C, Garrett D, House RK, Knapp D, Wiczcerek DJ, Verhey LJ. Description and dosimetric verification of the PEREGRINE Monte Carlo dose calculation system for photon beams incident on a water phantom. *Med Phys.* 2001 Jul;28(7):1322-37.
3. DeMarco JJ, Solberg TD, Smathers JB. A CT-based Monte Carlo simulation tool for dosimetry planning and analysis. *Med Phys.* 1998 Jan;25(1):1-11.
4. Rogers DW, Bielajew AF. Monte Carlo techniques of electron and photon transport for radiation dosimetry. *Dosimetry of Ionization Rad.* 1990;3:427-539.
5. Verhaegen F, Seuntjens J. Monte Carlo modelling of external radiotherapy photon beams. *Phys Med Biol.* 2003 Nov 7;48(21):R107-64.
6. Sheikh-Bagheri D, Rogers DW, Ross CK, Seuntjens JP. Comparison of measured and Monte Carlo calculated dose distributions from the NRC linac. *Med Phys.* 2000 Oct;27(10):2256-66.
7. Mackie TR, Kase K, Bjarngard B, Attix FH. Application of the Monte Carlo method in radiotherapy dosimetry of ionizing radiation. 1990;3:541-620.
8. Rogers DW, Faddegon BA, Ding GX, Ma CM, We J, Mackie TR. BEAM: a Monte Carlo code to simulate radiotherapy treatment units. *Med Phys.* 1995 May;22(5):503-24.
9. Ahnesjö A, Aspradakis MM. Dose calculations for external photon beams in radiotherapy. *Phys Med Biol.* 1999 Nov;44(11):R99-155.
10. Sievinen J, Ulmer W, Kaissl W. AAA photon dose calculation model in Eclipse. Palo Alto (CA): Varian Medical Systems. 2005.
11. Rogers DWO, Ma CM, Ding GX, Walters B, Sheikh-Bagheri, D, Zhang GG. BEAMnrc User's Manual. National Research Council Report PIRS 509a (rev F). 2001.
12. Ma CM, Rogers DWO, Walters B. DOSXYZnrc User's Manual. National Research Council Report PIRS 509b (rev F). 2001.
13. Treurniet, JA, Walters BRB, Rogers DWO. BEAMnrc, DOSXYZnrc and BEAMDP GUI User's Manual. National Research Council Report PIRS 0623(rev B). 2001.
14. Johns HE, Cunningham JR. *The Physics of Radiology.* (4th edition); 1983.
15. Van Dyk J. *The Modern Technology of Radiation Oncology: A Compendium for Medical Physicists and Radiation Oncologists.* Medical Physics Publishing; 1999.
16. Khan FM. *The Physics of Radiation Therapy.* Lippincott Williams & Wilkins. (3 edition); 2003.
17. Vazquez-Quino LA, Massingill B, Shi C, Gutierrez A, Esquivel C, Eng T, Papanikolaou N, Stathakis S. Monte Carlo modeling of a Novalis Tx Varian 6 MV with HD-120 multileaf collimator. *J Appl Clin Med Phys.* 2012 Sep 6;13(5):3960.
18. Yang J, Li J, Chen L, Price R, McNeeley S, Qin L, Wang L, Xiong W, Ma CM. Dosimetric verification of IMRT treatment planning using Monte Carlo simulations for prostate cancer. *Phys Med Biol.* 2005 Mar 7;50(5):869-78.
19. Othman IE, Khalifa RS, Elsariti A. Electron Beam Characteristics and Dose Profiles of 9 MeV Varian Clinac 2100C/D Linear Accelerator Using OMEGA BEAMnrc Code System. *J. of Science.* 2022;15:37-45.
20. Othman I, Abour B, Alsnozi Z. Non-Uniform Spatial Dose Distributions Around Co-60 in Human Tissue for Brachytherapy Treatment using Monte Carlo EGS Code. *Alq J Med App Sci.* 2022;5(2):396-405. <https://doi.org/10.5281/zenodo.6892393>.
21. Othman IE, Amer M. Non-Uniform Spatial Dose Distributions Around Ir-192 for Treating Oral Cavity in Brachytherapy using Monte Carlo EGS Code. *ICTS2019.* 4-6 March 2019.
22. Othman IE, Elgemaey MA. A study of Photon Beam Characteristics, Dose Profiles and Isodose curves of 6 MV Varian Clinac 600C Linear Accelerator Using OMEGA BEAMnrc Monte Carlo Code System. 14 th Arab Conference on the Peaceful Uses of Atomic Energy, Sharm El-Sheikh, Arab Republic of Egypt. 16-20 December 2018.
23. Othman IE, Abuzariba SM, El-Doppati RM. Radiotherapy Treatment Planning of 16 MV X-Ray Linear Accelerator Using OMEGA BEAMnrc Monte Carlo Code System. *The First Annual Conference on Theories and Applications of Basic and Biosciences.* 2017:331-337.

24. Rogers DW, Walters B, et al. BEAMnrc User's Manual. Report PIRS 0509. 2007.
25. Rogers DW, Faddegon BA, Ding GX, Ma CM, We J, Mackie TR. BEAM: a Monte Carlo code to simulate radiotherapy treatment units. Med Phys. 1995 May;22(5):503-24.
26. Rogers, DW, Walters B, et al. DOSXYZnrc User's Manual. Report PIRS 794. 2004.
27. Kawrakow I, Mainegra-Hing E, Rogers DWO, Tessier F, Walters BRB. The EGSnrc Code System: Monte Carlo Simulation of Electron and Photon Transport. NRCC Report PIRS-0701. 2009. 310.

## مقارنة خصائص قياس الجرعات لشعاع الإلكترون 6 MeV إلى 9 MeV في المسرع الخفي Varian Clinac 2100C/D باستخدام نظام كود OMEGA-BEAMnrc Monte Carlo

ابراهيم عثمان\* , ابراهيم سليم

قسم تقنية الإشعاع، كلية التقنية الطبية، جامعة الجفرة، هون، ليبيا

### المستخلص

**الأهداف.** يوضح هذا العمل الاختلافات بين أوضاع شعاع الإلكترون 6 MeV و 9 MeV في المسرع الخفي Varian Clinac 2100CD (Linac) من خلال فحص بيانات قياس الجرعات الخاصة بهم. **طرق الدراسة.** تخطيط العلاج المستخدم هنا هو نظام كود مونت كارلو OMEGA-BEAMnrc (MC)، والذي يستخدم على نطاق واسع لتحسين المعدات المختلفة المستخدمة في العلاج الإشعاعي. في العمل الحالي، تمت محاكاة Linac المذكور أعلاه باستخدام نظام الكود BEAMnrc MC لإنتاج ملف فضاء طور 10 × 10 سم لشعاع إلكتروني 6 MeV. تمت نمذجة ومحاكاة الأطياف المنتجة لمساحة طور الشعاع والتي قدمتها الوكالة الدولية للطاقة الذرية (IAEA) لشعاع الإلكترون بمجال رؤية 10 × 10 سم، وتمت محاكاتها وتحليلها أخيراً باستخدام BEAMdp خصائص الشعاع التي تمت دراستها هنا هي، التدفق، تدفقات الطاقة، متوسط الطاقة والتوزيع الزاوي والطيفي لمكونات الحزمة، الفوتونات، الإلكترونات، البوزيترونات والمجموع الكلي (جميع المكونات). تم نقل حزم الإلكترون المنتجة في فاننوم مائي باستخدام كود DOSXYZnrc وتم حساب الجرعة الممتصة للمحور المركزي وملامح الشعاع ومنحنيات الأيزودوس. تم تحليل منحنيات الجرعة العميقة للمحور المركزي وملامح الجرعة ومنحنيات الأيزودوس لحزم الإلكترون في فاننوم الماء باستخدام كود DOSXYZnrc و STATDOSE و DOSXYZ\_SHOW. **النتائج.** تمت مقارنة نتائج هذه الدراسة لحزمة 6 MeV مع تلك التي تم نشرها سابقاً لحزمة 9 MeV. أظهرت هذه الدراسة أن العمق عند الجرعة القصوى dmax لشعاع 9 MeV أعلى من ذلك لـ 6 MeV في حين أن كلا الملفين لهما نفس الاتجاه. يمكن لنظام الكود OMEGA-BEAMnrc إنشاء ملفات بيانات مساحة الطور بدقة وهي مماثلة لتلك التي توفرها بيانات الوكالة الدولية للطاقة الذرية. **الخاتمة.** يمكن لنظام Omega Beam Code محاكاة المسرع الخفي السريري لإنتاج شعاع إلكترون الذي يمكن استخدامه لتوليد توزيعات دقيقة لجرعة MC في فاننوم الماء أو في المرضى من أجل تحسين المعدات في العلاج الإشعاعي ولأغراض قياس الجرعات الإشعاعية.

**الكلمات الدالة.** قياس الجرعات الإشعاعية، مونت كارلو أو ميغا BEAMnrc، ملف مساحة الطور، ملفات تعريف الجرعة، منحنيات الأيزودوس.